

Encapsulated solid phase epitaxy of a Ge quantum well embedded in an epitaxial rare earth oxide

Apurba Laha^{1,3}, E Bugiel¹, M Jestremski¹, R Ranjith¹,
A Fissel² and H J Osten¹

¹ Institute of Electronic Materials and Devices, Leibniz University of Hannover, Appelstrasse 11A, D-30167 Hannover, Germany

² Information Technology Laboratory, Leibniz University of Hannover, Schneiderberg 32, D-30167 Hannover, Germany

E-mail: laха@mbe.uni-hannover.de

Received 23 September 2009, in final form 12 October 2009

Published 29 October 2009

Online at stacks.iop.org/Nano/20/475604

Abstract

An efficient method based on molecular beam epitaxy has been developed to integrate an epitaxial Ge quantum well buried into a single crystalline rare earth oxide. The monolithic heterostructure comprised of Gd_2O_3 –Ge– Gd_2O_3 grown on an Si substrate exhibits excellent crystalline quality with atomically sharp interfaces. This heterostructure with unique structural quality could be used for novel nanoelectronic applications in quantum-effect devices such as nanoscale transistors with a high mobility channel, resonant tunneling diode/transistors, etc. A phenomenological model has been proposed to explain the epitaxial growth process of the Ge layer under oxide encapsulation using a solid source molecular beam epitaxy technique.

(Some figures in this article are in colour only in the electronic version)

1. Introduction

Recent years have witnessed an aggressive approach to scaling down complementary metal oxide semiconductor (CMOS) devices, which have been the backbone of the information technology revolution [1]. Governed by the dogmatic Moore's law, today's transistor, which is the building block of all integrated circuits has reached its smallest possible dimension that could so far be fabricated with classical materials such as Si based gate dielectrics with Si acting as the channel [2, 3]. To continue this decade-long scaling tradition, the semiconductor industry is now desperately looking for new solutions that could survive at least for the next decade. Researchers around the world have come up with several possible solutions. However, only a very few among them might eventually deliver a viable technology. This is due to the fact that, to implement such a concept, industry needs to set up a brand new CMOS technology, which has never been welcomed due to the very high cost factor. Therefore, any solution that could shortly be realized within existing CMOS technologies may at least at the moment have an edge over any other radical concepts

such as electronic spin based transistors (spintronics) and the computation based on quantum mechanical phenomena (quantum computation), etc [4–6].

At present, the replacement of Si based gate dielectrics with high dielectric constant oxides (high- k) such as HfO_2 , Gd_2O_3 , etc together with high mobility channel materials such as Ge, III–V semiconductor on Si substrates has been proven to be extremely promising for next generation CMOS devices on the laboratory scale [7–9]. One of the greatest advantages of such an approach is that it could just be implemented to the ongoing CMOS technology with mere modification.

The concept of silicon-on-insulator (SOI) CMOS technology has been very successful in the modern semiconductor industry due to its 20–30% higher performance over bulk CMOS technology [10]. Recently, many research groups as well as industries have preferred to use Ge as a channel material due to its higher mobility than Si [11, 12]. In particular, a compressively strained Ge channel exhibits significant enhancement of hole mobility [13, 14]. Moreover, Ge-on-insulator (GOI) has been highlighted for the GOI CMOS concept due to the higher Ge mobility compared to Si [15]. However, growing single crystalline GOI has been quite a

³ Author to whom any correspondence should be addressed.

difficult task due to energetic incompatibility corresponding to the crystal growth process. A few approaches such as surfactant mediated epitaxial growth at higher temperature [16], Ge condensation [17], and a tedious approach based on a multi-step *in situ* and *ex situ* heating treatment [18] have been successful in growing a crystalline Ge layer on some high- k oxides and SiO₂. However, in all the reports the structures showed a thick amorphous interfacial layer appearing between the high- k oxide and the substrate during these processes. Furthermore, embedding single crystalline Ge into crystalline high- k oxide remains a tedious job due to several constraints associated with the epitaxial growth. As of now, there are very few reports on the successful growth of an epitaxial Ge layer embedded into crystalline high- k oxides. However, such an oxide–Ge–oxide epitaxial heterostructure could possess potential applications in various quantum-tunneling devices for very low power applications.

In the present work we have developed a monolithic and efficient approach to integrate an epitaxial Ge layer into an epitaxial rare earth oxide such as Gd₂O₃. Being an epitaxial host matrix, Gd₂O₃ adds up many unique advantages that could never be realized with an amorphous matrix. Furthermore, today's technological demands not only require an implementation of high mobility channel materials but also high- k oxide as the gate dielectric to sustain the dogmatic scaling path for at least the next decade [19].

Another prospective application of such a heterostructure could be in resonant tunneling devices where the mechanism of quantum mechanical tunneling could be utilized to realize a new type of device that could play a pivotal role in the post-CMOS era [20]. A double barrier Ge quantum well with epitaxial Gd₂O₃ as the potential barrier on both sides could be used for a robust resonant tunneling device, which could, in principle, be useful for room temperature operation.

2. Experimental details

All experiments were performed in an integrated multichamber molecular beam epitaxy (MBE) system. The preparation method consists of three principal steps: firstly, an epitaxial Gd₂O₃ was deposited on p-Si(111) ($1\text{--}10 \Omega \text{ cm}$) substrates. The substrate temperature during deposition was maintained at 650 °C while the oxygen partial pressure was kept at 5×10^{-7} mbar. The details of Gd₂O₃ deposition on different Si substrates were described elsewhere [21]. The next step is to deposit a Ge layer on the epi-Gd₂O₃ surface. The higher temperature ($>150^\circ\text{C}$) deposition of Ge on the oxide surface results in island formation due to the higher surface free energy of Ge and the large mobility of Ge adatoms on epi-Gd₂O₃ surfaces. To avoid any Ge island formation, the substrate temperature was reduced to 30 °C and subsequently the deposition of amorphous Ge was carried out. Reduction of the substrate's temperature brings down the mobility of Ge adatoms significantly and hence the inter-atomic interaction between oxide and Ge surface atoms dominates over intra-atomic interaction among Ge atoms. The deposition temperature and the rate for the Ge layer certainly play a critical role in accomplishing two-dimensional (2D)

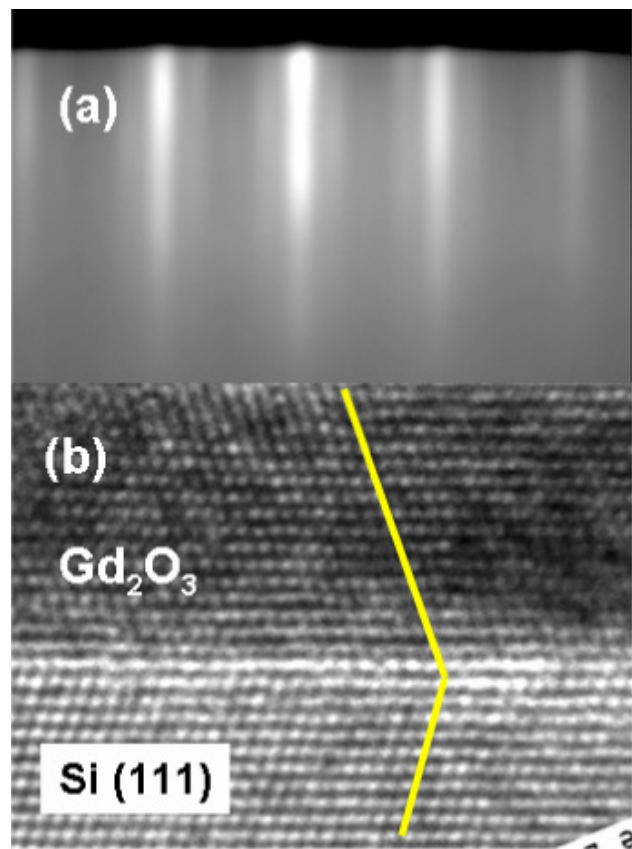


Figure 1. (a) RHEED image of Gd₂O₃ thin film deposited at 650 °C on Si(111) substrate. (b) Cross-sectional HRTEM image of epitaxial Gd₂O₃ along the <110> zone axis.

layer formation on the Gd₂O₃ surface. The detailed growth mechanism will be discussed in section 3. The following is the third and final step, which is the most critical and important stage of the growth sequences. After the growth of the amorphous Ge layer, the substrate temperature was ramped up to 650 °C with a ramp rate of 100 °C min⁻¹. During this ramp-up process, the Ge layer was encapsulated by depositing Gd₂O₃ at a rate of 0.6 nm min⁻¹ and this was already started at 100 °C. When the substrate temperature reached 600 °C, oxygen partial pressure in the chamber was increased to 5×10^{-7} mbar. An analogous method was reported recently by Fissel *et al* for the growth of a Si based nanostructure [22].

The structural evolution of the heterostructure was monitored *in situ* by reflection high-energy electron diffraction (RHEED), and *ex situ* by high-resolution x-ray diffraction (HRXRD), and high-resolution transmission electron microscopy (HRTEM) using a JEM 2100F microscope with an ultrahigh-resolution objective operating at 200 kV.

3. Results and discussions

MBE offers a unique advantage of monitoring the evolution of crystal growth from the very early stage. In the present study, we have used the real time *in situ* RHEED technique to monitor the evolution of the growth mode at various stages. Figure 1(a) shows the RHEED image of a Gd₂O₃ thin film deposited at

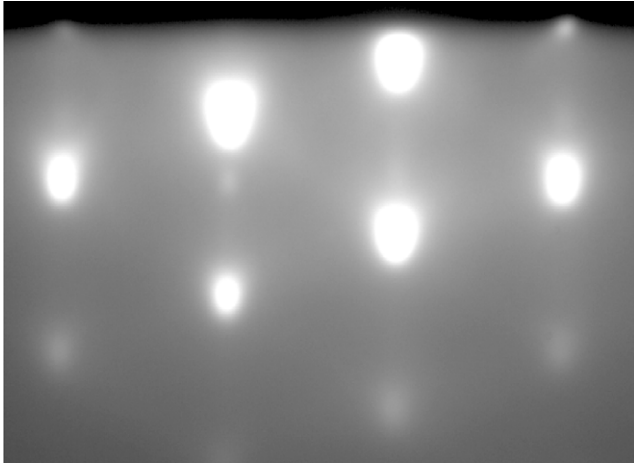


Figure 2. RHEED image of Ge islands grown on a single crystalline Gd_2O_3 surface at 600°C .

650°C on an Si(111) substrate. The streaky lines together with the substreaks confirm that a well-ordered and high quality 2D layer was epitaxially grown. Epitaxial growth of Gd_2O_3 on Si substrate was further confirmed by cross-sectional HRTEM (shown in panel (b) of the same figure), which also shows that Gd_2O_3 exhibits a twinning relationship (A/B) along the surface normal with the underlying Si substrate. A detailed study of oxide growth on different Si substrates can be found elsewhere [21, 22].

Having established the deposition conditions for epitaxial growth of the oxide layer, we carried out the growth of the Ge layer on an epitaxial oxide surface, which is the principal task of the present work. The growth of Ge on an epi- Gd_2O_3 surface cannot be achieved by conventional epitaxy techniques because the higher surface free energy of Ge with respect to Gd_2O_3 gives rise to island growth on the oxide surface at higher temperature ($>150^\circ\text{C}$) [23]. Figure 2 shows an example of Ge island growth on a single crystalline Gd_2O_3 surface using conventional epitaxy at 600°C . Furthermore, RHEED images of Ge islands on the epitaxial oxide surface deposited at 600°C infer that a straightforward high temperature deposition of Ge on the oxide surface does not result in an epitaxial 2D layer. Therefore, an alteration of the process steps is called for. However, to prove whether the surface energetics solely determine the growth mode, we carried out growth of a Gd_2O_3 layer on a Ge layer, which was grown on a Si substrate using surfactant mediated epitaxy technique [24]. Here we observed a well-ordered and 2D epitaxial growth under similar growth condition, as shown in figure 3. Streaky RHEED patterns along with HRTEM images confirm that epitaxial Gd_2O_3 can be grown on the Ge surface using the epitaxy technique, details can be found elsewhere [25].

Based on the experimental evidence described above, the following process steps have been carried out in order to achieve a Ge epitaxial layer on an oxide surface. As described in section 2, conventional epitaxy does not work for Ge layer growth on an oxide surface, the only viable solution available in the present case is to reduce the surface free energy of the Ge layer. Furthermore, the reduction of the deposition

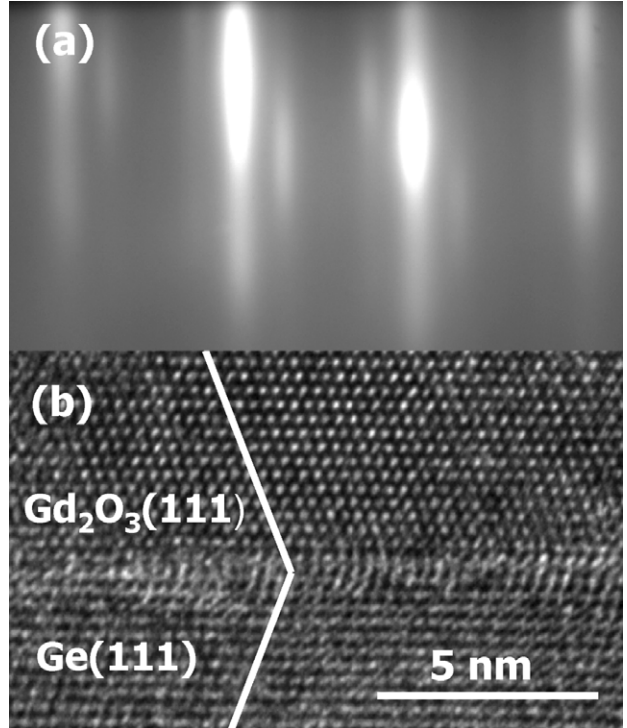


Figure 3. (a) RHEED image of an epitaxial Gd_2O_3 layer deposited at 600°C on a Ge(111) substrate. (b) Cross-sectional HRTEM image of epitaxial Gd_2O_3 on Ge(111) along the $\langle 110 \rangle$ zone axis.

temperature alone does not make any difference. Any attempt to crystallize the amorphous layer (i.e. to perform a solid phase epitaxy [26, 27]) leads again to islanding. Consequently, we developed an unconventional method to accomplish an epitaxial Ge layer buried into a crystalline rare earth oxide. We call this process '*encapsulated solid phase epitaxy (ESPE)*'.

The detailed process steps have been described in section 2. In this section we will describe a phenomenological model, which eventually helps us to understand the mechanism of encapsulated Ge epitaxy in the present study. However, before we proceed to such a discussion, we present a comprehensive investigation of the structural quality of such a heterostructure both in macro- and microscopic dimensions to establish the viability of our approach. Figures 4(a) and (b) compare the RHEED images of the uppermost Gd_2O_3 layers deposited on Ge layers, which were deposited on an epi- Gd_2O_3 surface at 50°C and 30°C , respectively, depicting how critical the deposition temperature of the Ge layer is. In the former case, the surface of the top oxide layer was quite rough, yielding spotty RHEED images and exhibiting an almost island-like kind of growth. However, in the latter case, a very smooth 2D layer was observed. It should be mentioned here that except for the substrate temperature during Ge deposition, all other parameters during the above process were kept similar. Further, it turns out that the Ge layer deposited at and above 50°C becomes poly/microcrystalline, resulting in a quite rough surface, which might lead to the rough top oxide layer as evidenced by the RHEED pattern and x-ray reflectivity measurements (not shown). This could

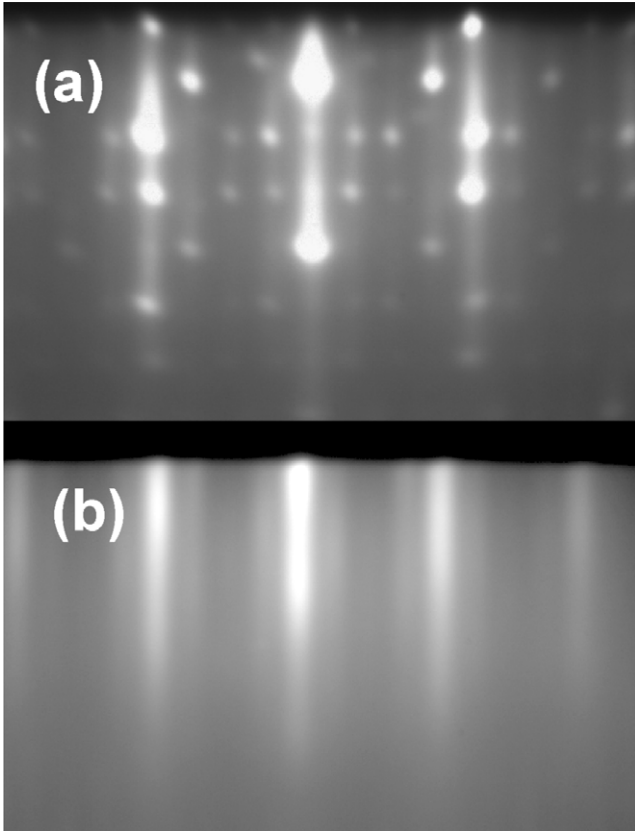


Figure 4. RHEED images of the top Gd_2O_3 on Ge layer deposited during the temperature ramp-up process started at 100–650 °C, shown schematically in figure 9. The image has been taken after completion of deposition. The only difference here is the deposition temperature of the underlying Ge layer onto the epi- Gd_2O_3 surface. In the former case (a) the Ge layers were deposited at 50 °C, while in the latter (b) the layer was deposited at 30 °C.

be attributed to the higher surface mobility of Ge adatoms at higher temperature (>50 °C) on the epi-oxide surface [28].

Following the preliminary *in situ* examination of the heterostructures using RHEED, we carried out high-resolution x-ray diffraction (HRXRD) studies to elucidate the global crystalline quality of the structure. Figure 5 compares the HRXRD patterns of Gd_2O_3 –Ge– Gd_2O_3 heterostructures grown on Si(111) substrates with varying germanium thickness. The diffraction patterns of the heterostructures clearly show the thickness fringes around the average out-of-plane lattice spacing of Ge(111). The average lattice plane reflection and the thickness fringes observed around the same, indicate the presence of atomically sharp interfaces among the layers present in the heterostructures, in accordance with the dynamical theory of x-ray scattering [29, 30].

The epitaxial quality was further analyzed by x-ray rocking curve analysis. Figure 6 compares the x-ray rocking curve analysis around the out-of-plane lattice reflection of the Ge(111) planes of thicknesses 6.5 nm, 13.45 nm, and 35.45 nm, respectively. The measured full width at half maximum (FWHM) of the rocking curve peaks for the heterostructures with Ge thicknesses of 6.5, 13.45, and 35.45 nm were 208, 206, and 204 arcsec, respectively. The

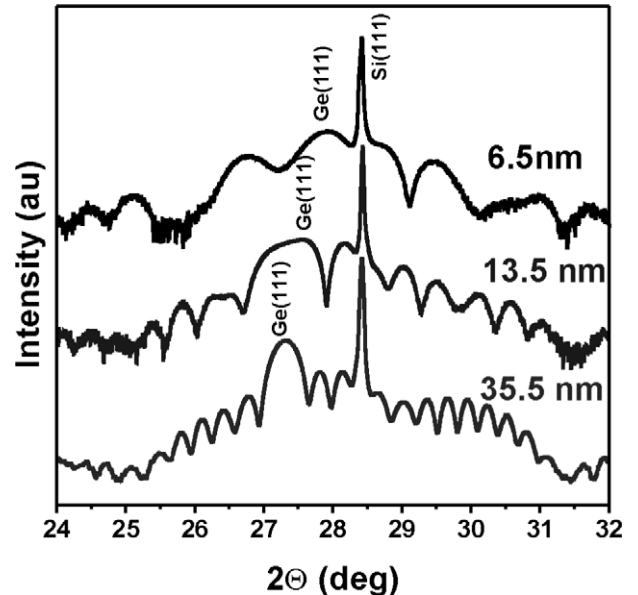


Figure 5. High-resolution x-ray diffraction (HRXRD) patterns of Gd_2O_3 –Ge– Gd_2O_3 heterostructures grown on Si(111) substrates with varying germanium thickness.

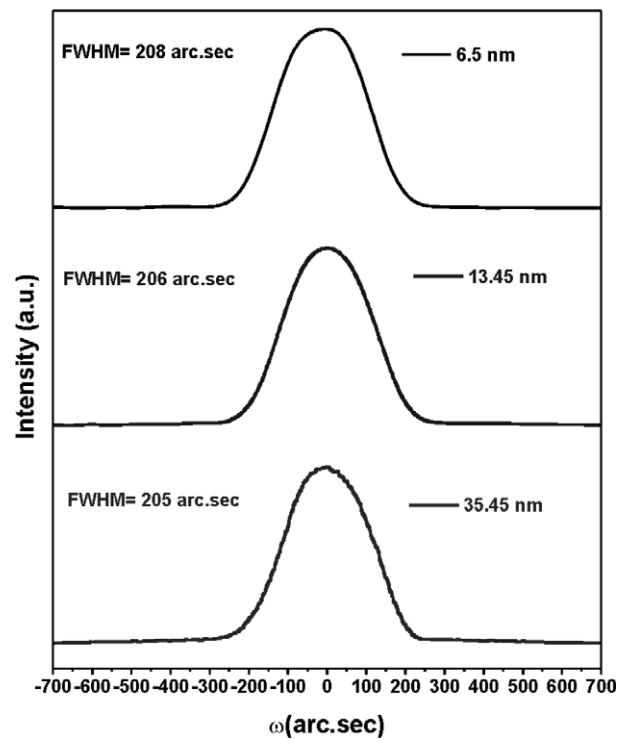


Figure 6. X-ray rocking curves around the out-of-plane lattice reflection of the Ge(111) plane for thicknesses of 6.5 nm, 13.45 nm, and 35.45 nm, respectively.

observed small values of the widths clearly depict an excellent layer quality, almost independent of the germanium layer thickness. In epitaxial layers, the full width at half maximum (FWHM) of the x-ray rocking curves originates from the strain field associated with the threading dislocation density and the lattice mismatch. In the present case, however, small FWHM

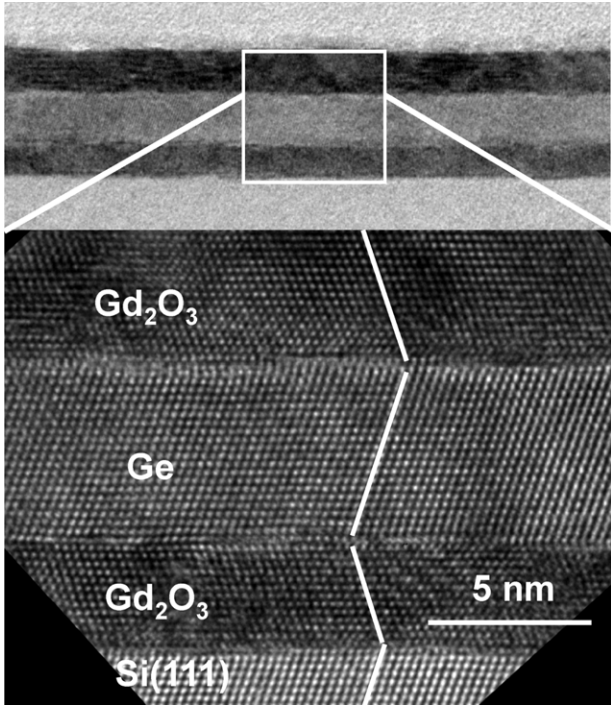


Figure 7. Cross-sectional HRTEM image of the Gd_2O_3 -Ge- Gd_2O_3 heterostructure with a 6.5 nm thick Ge layer.

values observed even for thicker layers can be attributed to the presence of a low strain field arising from very low defect densities. Figure 7 shows the cross-sectional HRTEM image of the Gd_2O_3 -Ge- Gd_2O_3 heterostructure with a 6.5 nm thick Ge layer taken along the $\langle 110 \rangle$ zone axis. The micrograph reveals the structural perfection of the heterostructure under investigation, grown by encapsulated solid phase epitaxy. The atomic steps visible at the substrate surface could be seen to be reproduced at the other two interfaces, depicting the

atomically sharp interfaces. The enlarged images of the three interfaces ($i-1$, $i-2$, $i-3$) shown in figures 8(a) and (b) once again qualitatively prove the quality of the same both beneath and above the Ge layer. What could be seen beyond doubt is that despite having a relatively large lattice mismatch with the oxide host matrix, the single crystalline Ge layer could be encapsulated fairly well without any defect penetrating into other parts of the heterostructure. Nevertheless, there may be some dislocations pertaining to the lattice mismatch at the epi-interfaces. However, based on the comprehensive investigation described above, we can apparently conclude that these defects are mostly confined to the interface region. One of the reasons for accomplishing such high quality heterostructures could be attributed to the differences in space group of the host oxide matrix ($Ia3$) with Ge. Hence, the atomic arrangement at the oxide layer surface is strikingly different from that of Ge ($Fd3m$) at the interfaces. The crystallization of the encapsulated Ge layer during the temperature ramp-up process evolves from the bottom interface ($i-1$). The epitaxial Gd_2O_3 layer acts as a seeding layer and consequently forces the crystallization process of a few monolayers above it. Subsequently, the crystallization process propagates upwards and finally to the encapsulating Gd_2O_3 layer. Figure 9 describes the schematic representation of the whole process that takes place during crystallization of such heterogeneous systems under such conditions. The process starts with epitaxial growth of the Gd_2O_3 layer and finally ends up with the epitaxial growth of another oxide layer.

3.1. Encapsulated solid phase epitaxy

To understand the physics of the encapsulated solid phase epitaxy let us start with two classical modes of growth processes. Based on the phenomenological model; two extreme cases of growth modes, i.e. ‘layer by layer’ and ‘island

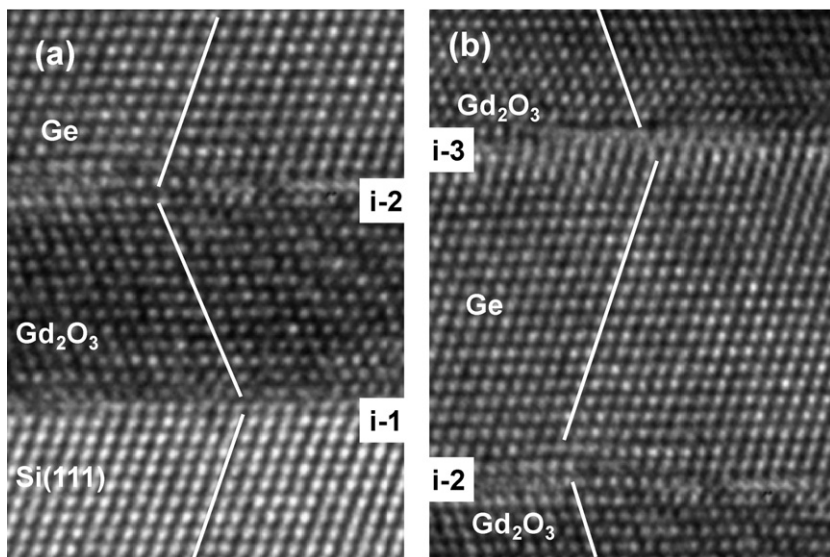


Figure 8. Enlarged cross-sectional HRTEM images of the Gd_2O_3 -Ge- Gd_2O_3 heterostructure on the Si(111) substrate depicting atomically sharp interfaces with distinct evidence of the atomic steps. The encapsulated Ge layer has undergone thermal annealing during the temperature ramp-up process and subsequently during the deposition of the top Gd_2O_3 layer at 650 °C.

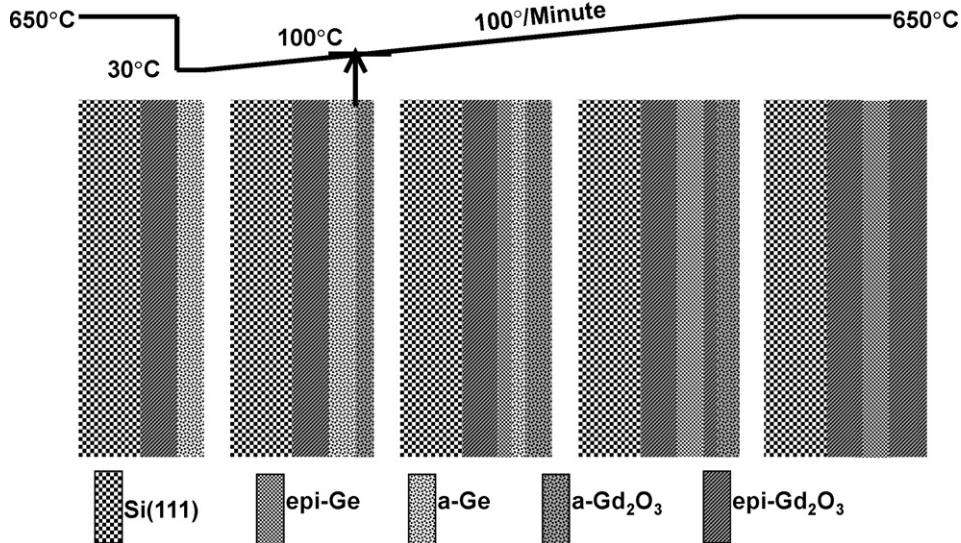


Figure 9. Schematic representation of the three-step growth process that was developed to obtain a Gd_2O_3 – Ge – Gd_2O_3 heterostructure on an $\text{Si}(111)$ substrate.

growth', can be observed under the following thermodynamic conditions [31].

For layer growth:

$$\gamma_s \geq \gamma_F + \gamma_{F/S} - Ck \ln(p/p_0). \quad (1)$$

For island growth:

$$\gamma_s < \gamma_F + \gamma_{F/S} - Ck \ln(p/p_0) \quad (2)$$

where γ is the free energy, and subscripts S, F, and F/S correspond to substrate, film, and film–substrate interface. p/p_0 represents the degree of 'supersaturation'; the driving force for the formation of a thin film deposited from an ambient vapor phase and C is a constant, k is the Boltzmann constant.

In the case of an encapsulated Ge layer, the ambient is the solid phase Gd_2O_3 that is wetting the underlying Ge layer because of its lower surface free energy compared to the Ge layer. Due to this wetting, the Ge layer has no open free surface and, hence, the interaction between neighboring Ge atoms at the surface will be significantly limited. Now, if we consider the interface between the overgrown Ge and underlying Gd_2O_3 , (interface i —2) the epitaxial growth of solid phase Ge will be significantly perturbed.

In a conventional solid phase epitaxy, the system under investigation is considered to be an open system. Therefore, the surface free energy of the Ge layer (system under consideration) could be written as [32]

$$dF^s = -S^s dT + \sigma^s dA + \sum_i \mu_i^s dn_i^s \quad (3)$$

where F^s is the surface free energy or the Helmholtz surface free energy, S^s is the entropy of the surface and σ^s is the surface tension, μ_i^s and n refer to the chemical potential and number of moles of the i th species of Ge atoms at the surface respectively. 's' corresponds to the surface.

Integrating equation (3) gives:

$$\gamma^s = -s^s T + \sigma^s + \sum_i \Gamma_i \mu_i^s \quad (4)$$

$$\text{where } \gamma^s = \frac{F}{A}, s = \frac{S^s}{A}, \text{ and } \Gamma_i = \frac{n_i^s}{A}.$$

During encapsulated solid phase epitaxy, the number of molecule/atoms at the Ge surface can be considered as constant ($dn_i^s = 0$), however, the intermolecular interaction between the adatoms and surface atoms will have a significant impact on the free energy (F) of the surface. Therefore, equation (3) could be written as

$$dF_e^s = -S^s dT + \sigma^s dA - \sum_j \chi_{ij} dn_j^o \quad (5)$$

and after integration:

$$\gamma_e^s = -s^s T + \sigma - \sum_{i,j}^{i \neq j} \chi_{ij} N_j^o. \quad (6)$$

F_e^s and γ_e^s are the surface free energy and energy per unit area of the encapsulated Ge surface. 'j' corresponds to a certain adatom or molecule of Gd_xO_y on the Ge surface and certainly will have an interaction with the i th atom within the Ge surface. χ refers to the parameter that corresponds to intermolecular forces. The intermolecular exchange interaction reduces the Ge surface free energy in the present case because of the attractive van der Waals force (intermolecular force). N^o is the number of adatoms on the Ge surface, where 'o' refers to the oxide bond to the Ge surface.

If we now compare the equations (4) and (6), it appears that the surface free energy of the encapsulated layer has been reduced due to an intermolecular exchange interaction. Furthermore, the change of surface free energy due to chemical potential could be omitted for the constant number of atoms/molecules on the Ge surface. Decreasing the surface

free energy under encapsulation fairly satisfies the condition for layer growth (equation (1)) of Ge on the epi-Gd₂O₃ surface and, therefore, results in a 2D, smooth and epitaxial Gd₂O₃–Ge–Gd₂O₃ heterostructure.

4. Summary

In summary, an efficient method (called encapsulated solid phase epitaxy (ESPE)) has been successfully developed to grow an epitaxial heterostructure based on Gd₂O₃–Ge–Gd₂O₃ on Si(111) substrates. The monolithic structure reveals excellent crystalline quality and could be used for many applications in future quantum-effect devices. A simple model based on phenomenological understanding has been provided to explain the process of ESPE.

References

- [1] Semiconductor Industry Association 2003 *International Technology Roadmap for Semiconductors* available at <http://public.itrs.net>
- [2] Jeong M, Doris B, Kedzierski J, Rim K and Yang M 2004 *Science* **306** 2057
- [3] Liu T-J K and Chang L 2009 *Transistor Scaling to the Limit Into The Nano Era (Springer Series in Materials Science* vol 106) (Berlin: Springer) p 191
- [4] Wolf S A, Chtchelkanova A Y and Treger D M 2006 *IBM J. Res. Dev.* **50** 101
- [5] Bennett C H 1995 *Phys. Today* **48** (10) 24
- [6] Bennett C H and DiVincenzo D P 2000 *Nature* **404** 247
- [7] Dimoulas A, Gusev E and McIntyre P C 2007 *Advanced Gate Stacks for High-Mobility Semiconductors (Springer Series in Advanced Microelectronics* vol 17) (Berlin: Springer)
- [8] Wilk G D, Wallace R M and Anthony J M 2001 *J. Appl. Phys.* **89** 5243
- [9] Hong M, Kwo J, Kortan A R, Mannaerts J P and Sergent A M 1999 *Science* **283** 1897
- [10] Colinge P 1991 *Silicon-on-Insulator Technology: Materials to VLSI* (Dordrecht: Kluwer Academic)
- [11] Toriumi A, Tabata T, Lee C H, Nishimura T, Kita K and Nagashio K 2009 *Microelectron. Eng.* **86** 1571
- [12] Krishnamohan T, Krivokapic Z, Uchida K, Nishi Y and Saraswat Krishna C 2006 *IEEE Trans. Electron Devices* **53** 990
- [13] Fischetti M V and Laux S E 1996 *J. Appl. Phys.* **80** 2234
- [14] Shang H, Okorn-Schmidt H, Ott J, Kozlowski P M, Steen S, Jones E C, Wong H-S P and Haensch W E 2003 *IEEE Electron Device Lett.* **24** 242
- [15] Preisler E J, Guha S, Perkins B R, Kazazis D and Zaslavsky A 2005 *Appl. Phys. Lett.* **86** 223504
- [16] Bojarczuk N A, Copel M, Guha S, Narayanan V, Preisler E J, Ross F M and Shang H 2003 *Appl. Phys. Lett.* **83** 5443
- [17] Nakaharai S, Tezuka T, Hirashita N, Toyoda E, Moriyama Y, Sugiyama N and Takagi S 2009 *J. Appl. Phys.* **105** 024515
- [18] Giussani A, Rodenbach P, Zaumseil P, Dabrowski J, Kurps R, Weidner G, Müssig H-J, Storck P, Wollschläger J and Schroeder T 2009 *J. Appl. Phys.* **105** 033512
- [19] Sugawara T, Oshima Y, Sreenivasan R and McIntyre P C 2007 *Appl. Phys. Lett.* **90** 112912
- [20] Rommel S L, Dillon T E, Dashiell M W, Feng H, Kolodzey J and Berger P R 1998 *Appl. Phys. Lett.* **73** 2191
- [21] Laha A, Osten H J and Fissel A 2006 *Appl. Phys. Lett.* **89** 143514
- [22] Fissel A, Kühne D, Bugiel E and Osten H J 2006 *Appl. Phys. Lett.* **88** 153105
- [23] Stekolnikov A A, Furthmüller J and Bechstedt F 2002 *Phys. Rev. B* **65** 115318
- [24] Wietler T F, Bugiel E and Hofmann K R 2005 *Appl. Phys. Lett.* **87** 182102
- [25] Wietler T F, Laha A, Bugiel E, Czernohorsky M, Dargis R, Fissel A and Osten H J 2009 *Solid-State Electron.* **53** 833
- [26] Copel M, Reuter M C, Kaxiras E and Tromp R M 1989 *Phys. Rev. Lett.* **63** 632
- [27] Osten H J, Klatt J, Lippert G, Dietrich B and Bugiel E 1992 *Phys. Rev. Lett.* **69** 450
- [28] Huang L, Liu F, Guang L H and Gong X G 2006 *Phys. Rev. Lett.* **96** 016103
- [29] Uragami T S 1971 *J. Phys. Soc. Japan* **31** 1141
- [30] Authier A 2003 *Dynamical Theory of X-Ray Diffraction (IUCR Monographs on Crystallography* vol 11) 2nd edn (Oxford: Oxford University Press)
- [31] Lüth H 2001 *Solid Surfaces, Interfaces and Thin Films* (Berlin: Springer)
- [32] Ip S W and Toguri J M 1994 *J. Mater. Sci.* **29** 688